# Preparation of Thermally Stable, Low Dielectric Constant, Pyridine-Based Polyimide and Related Nanofoams

## Elham Aram, Shahram Mehdipour-Ataei
Iran Polymer and Petrochemical Institute, Tehran, Iran
Correspondence to: S. Mehdipour-Ataei (E-mail: s.mehdipour@ippi.ac.ir)

**ABSTRACT:** Reaction of 6-chloronicotinoyl chloride with *p*-phenylene diamine resulted in preparation of a dichloro diamide compound. Subsequently, chloro displacement of this compound with 4-amino phenoxy groups led to production of a new pyridine-based ether diamine named as *N*,*N*′-(1,4-phenylene)bis(6-(4-aminophenoxy) nicotinamide). Novel polyimide was prepared through polycondensation reaction of the diamine with hexafluoroisopropylidene diphthalic anhydride (6-FDA) via two-step imidization method. In addition, new nanoporous polyimide films were produced through graft copolymerization of polyimide as the continuous phase with a thermally labile poly (propylene glycol) oligomer as the labile phase. The grafted copolymers were synthesized using reaction of the diamine and 6-FDA in the presence of poly (propylene glycol) 2-bromoacetate as thermally labile constituent via a poly(amic acid) precursor process. The labile block was decomposed via thermal treatment to release inert molecules that diffused out of the matrix to leave pores with diameters between 30 and 60 nm. The structures and properties of polyimide and polyimide nanofoams were characterized by different techniques including ^{1}H-NMR, FTIR, TGA, DMTA, SEM, TEM, dielectric constant, and tensile strength measurement. © 2012 Wiley Periodicals, Inc. J. Appl. Polym. Sci. 128: 4387–4394, 2013

## INTRODUCTION

In recent years, extensive research has been concentrated on the area of nanotechnology and nanomaterials with outstanding properties. Polyimide nanofoam is a representation of such advancement. Although polyimides have been utilized as electronic packages due to their excellent thermal, mechanical, and electrical properties,[1–7] their dielectric constants are insufficient to meet the requirement of interlayer dielectric. During the last years, many efforts have been achieved to prepare suitable aromatic diamines using them as building block for the preparation of high-performance polyimides. Improving various properties of the polyimides was one of the main objectives in this area.[8–18]

Different approaches to decrease dielectric constant of polyimides have been developed. The most common approach is the incorporation of pendant perfluoroalkyl groups.[19–22] This structural modification produces polyimide films with dielectric constants in the range of 2.4–2.7. There are some limitations on the preparation of fluoro-polyimides because of the synthetic difficulties associated with the fluorine-containing comonomers. Moreover, during the processing of fluorinated polymers evolution of HF has been observed causes the corrosion problems.

Reducing the dielectric constant of polyimides via introduction of silane unit into the backbone of polyimides is another method.[15] It is related to the reduced polarity of polyimides because of the incorporation of siloxane units into the polymer backbone. The dielectric constants of silane-containing polyimides (2.46–2.92) are lower than common siloxane-free polyimides (∼3).

An alternative approach to reduce the dielectric constant is to generate polyimide foams.[23,24] Polyimide foams have emerged as a high-performance cellular materials with big potential for applications in aerospace and microelectronic industries because of their excellent properties such as high thermal stability, good mechanical properties, and low dielectric constants.[25,26] The reduction in dielectric constant can be obtained by introducing voids into the film to benefit the low dielectric constant of air (dielectric constant of 1). Nanoporous polyimide films can be prepared from block or graft copolymers consisting of thermally stable (continuous phase) and thermally unstable (dispersed phase) blocks.[27,28] Upon thermal treatment, the labile block is eliminated by thermolysis, leaving pores with the size and shape of original copolymer morphology, i.e., on the tens of nanometer size scale. In this approach, it is critical to completely remove the labile block and generate uniform, controllable, and

closed pores. Also, the decomposition of labile block had to occur below the Tg of the polymer matrix. Moreover, the casting solvent must be effectively removed, prior to unstable block degradation, to prevent pores collapse.[6] Another important criterion for thermally labile coblock is finding a suitable synthetic route to well-defined functional oligomers and its subsequent quantitative decomposition into non-reactive species, which can readily diffuse through the polyimide matrix.

In this article, we report synthesis of thermally stable pyridine-based polyimide and their related nanofoams grafted with labile poly(propylene glycol). The morphology, dielectric constants, thermal, and physical properties of the pure polyimide and nanoporous polyimides were investigated.

## EXPERIMENTAL

### Materials

*p*-Phenylene diamine and bromoacetyl bromide were purchased from Merck Chemical. Hexafluoroisopropylidene diphthalic anhydride (6-FDA), 6-chloronicotinoyl chloride, poly(propylene glycol) mono butyl ether, and 4-aminophenol were obtained from Aldrich Chemical. 6-FDA was dried in a vacuum oven at 110°C for 8–10 h prior to use. *N*-Methyl-2-pyrrolidone (NMP) was purified under vacuum distillation in the presence of $CaH_2$.

### Instruments

Infrared measurements were performed on a Bruker-IFS 48 FTIR spectrometer (Ettlingen, Germany). The H-NMR spectra in a dimethyl sulfoxide (DMSO-$d_6$) or chloroform (CDCl$_3$) were recorded on a Bruker Avance DPX spectrometer operating at 400 MHz with tetramethylsilane as a reference. For elemental analyses, a Heraeus CHN–O rapid elemental analyzer (Wellesley, MA) was used. Thermogravimetric analysis (TGA) was carried out on a Polymer Lab TGA-1500 in air at a heating rate of 10°C/min. The dynamic mechanical measurements were performed with a polymer laboratories dynamic mechanical thermal analyzer (DMTA) and with a heating rate of 3°C/min (Surrey, UK). Inherent viscosities were measured with an Ubbelohde viscometer. Mechanical property was evaluated at room temperature on a tensile tester STM 20(SANTAM). Scanning electron microscopy (SEM) was obtained using a SEM XL30 (Philips, UK). Transmission electron microscopy (TEM) was performed on a TEM 208 S.Philips at 100 kV. The polymer samples were embedded in an aldrite resin and microtomed in cross section. The porosity of samples was determined by a Pascal 440 Porosimeter (Thermo Finnigan, Italy). The refractive indices of polymer films and nanoporous polymers were determined by the Metricon Prism Coupler Pc-2000 (Pennington, NJ) instrument. The number and weight average molecular weight ($M_n$ and $M_w$) were determined by gel permeation chromatography (GPC). It was performed on a Waters 150-C instrument using Styragel columns and a differential refractometer detector. The molecular weight calibration was carried out using polystyrene standards. Calibration and measurements were made at a flow rate of 1 mL/min, and DMF was used as solvent. A calibrated-density gradient column composed of water and calcium nitrate was used for measuring densities of polyimide and nanofoam films. Three samples were used for each density measurement.

### Monomer and Polymer Synthesis

**Synthesis of *N*,*N*´-(1,4-phenylene)bis(6-chloronicotinamide).** Into a 100-mL, two-necked, round-bottomed flask equipped with a calcium chloride drying tube, a nitrogen inlet tube, and a magnetic stirrer was placed 6.0 mmol (0.65 g) of *p*-phenylene diamine and 30 mL of dry NMP. The mixture was stirred at 0°C for 0.5 h. Then 38 mL triethylamine (TEA) and 12.5 mmol (2.27 g) of 6-chloronicotinoyl chloride were added to the mixture and the reaction mixture was stirred at 0°C for another 0.5 h. After completion of the addition, the temperature was raised to room temperature and stirred for 8 h. The reaction mixture was poured into water to give a solid, which was collected, washed thoroughly with methanol, and hot water. The obtained white solid precipitate was dried in a vacuum oven at 80°C (yield: 2.17 g, 93%). m.p. = 372–378°C. [IR (KBr): $\upsilon$ 3319, 3047, 1647, 1563, 1462, 1405, 1334, 1111, 822, and 673 cm$^{-1}$; $^1$H-NMR (DMSO-$d_6$): $\delta$ 10.48 (s, 2H, amide), 8.91 (d, 2H, pyridine), 8.31 (dd, 2H, pyridine), 7.72 (s, 4H, phenyl), 7.69 (d, 2H, pyridine); elemental analysis calculated for $C_{18}H_{12}Cl_2N_4O_2$ (M.W. = 387): C, 55.83%; H, 3.12%; N, 14.47%; found: C, 56.00%; H, 3.04%; N, 14.61%; Mass spectrum: m/e = 387.

**Synthesis of *N*,*N*´-(1,4-phenylene)bis(6-(4-aminophenoxy) nicotinamide).** Into a 100-mL, three-necked, round-bottomed flask equipped with a Dean-Stark trap, a condenser, a nitrogen inlet tube, a thermometer, an oil bath, and a magnetic stirrer was placed 10.0 mmol (3.87 g) of the dichloro compound, 50 mL of dry NMP, 25.0 mmol (2.78 g) of 4-aminophenol, and 35 mL of dry toluene. Then 33 mmol (4.56 g) of $K_2CO_3$ was added to the mixture, and the reaction mixture was heated to 140°C for 6 hr with continuous stirring. The generated water was eliminated from the reaction mixture by azeotropic distillation. The reaction temperature was raised to 165°C by the removal of more toluene and held at the same temperature for 20 hr. During this time, progress of the reaction was monitored by thin-layer chromatography. The mixture was allowed to cool and then poured into water. The precipitate was collected by filtration, washed repeatedly with 100 mL of 5% NaOH solution, hot water, and methanol. The gray solid product was dried in a vacuum oven at 60°C (yield: 4.79 g, 90%). m.p. = 384–389°C. [IR (KBr): $\upsilon$ 3427–3450, 3318, 3091, 1647, 1592, 1509, 1374, 1247, 1197, and 825 cm$^{-1}$; $^1$H-NMR (DMSO-$d_6$): $\delta$ 10.23 (s, 2H, amide), 8.66 (d, 2H, pyridine), 8.24 (dd, 2H, pyridine), 7.68 (s, 4H, phenyl), 6.95 (d, 2H, pyridine), 6.79 (d, 4H, phenyl), 6.58 (d, 4H, phenyl), and 5.01 (s, 4H, amine); elemental analysis calculated for $C_{30}H_{24}N_6O_4$ (M.W. = 532): C, 67.66%; H, 4.54%; N, 15.78%; found: C, 67.78%; H, 4.67%; N, 15.66%; Mass spectrum: m/e = 532.

**Preparation of Polyimide Film.** A 100-mL, two-necked flask, fitted with a nitrogen inlet was charged with 1.5 mmol (0.798 g) of diamine and 60 mL of dry NMP. After the flask was cooled to 5°C, 1.5 mmol (0.679 g) of 6-FDA was added to the mixture. The solution was heated up to room temperature and stirred for 24 h. Poly(amic acid) was precipitated into mixture of methanol/water (1:1 v/v); it was then filtered and dried in a vacuum oven at 40°C. The poly(amic acid) was subsequently converted to polyimide by thermal imidization process; so, poly(amic acid) was dissolved in NMP or dimethylacetamide (DMAC) at concentration of 7–10%
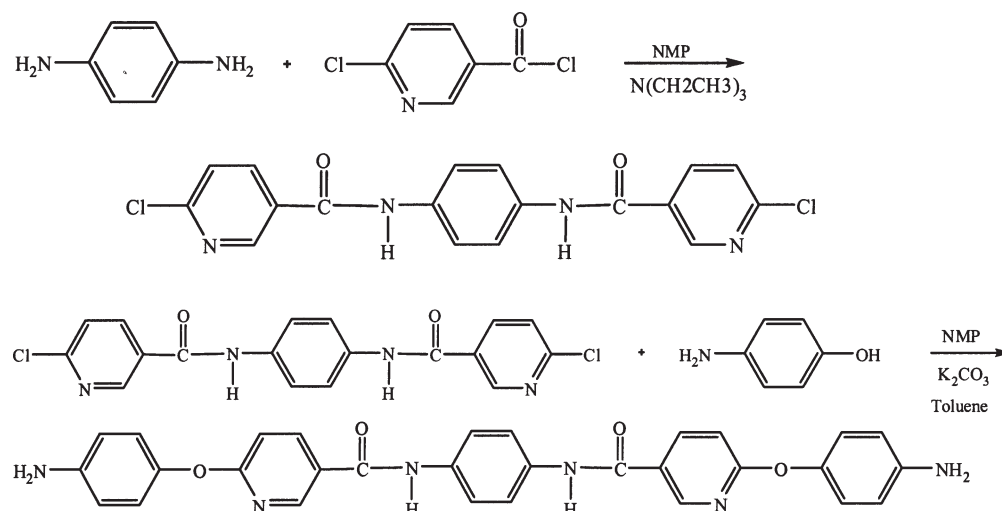
**Scheme 1.** Preparation of diamine.

solids. The solution was cast on a glass plate and heated incrementally to 180°C in an air atmosphere to remove the solvent and produce a fully imidized polyimide film.

**Synthesis of Poly(propylene glycol)-2-bromoacetate.** A typical preparation of poly(propylene glycol)-2-bromoacetate (PPG-Br), having a number–average molecular weight of ca. 1000 and 2500 g mol$^{-1}$, was as follows. A 100-mL flask was charged with 5 mmol of poly(propylene glycol) monobutyl ether (PPGOH-1000 (5.00 g), PPGOH-2500 (12.50 g), 5.5 mmol (0.561 g) of TEA, and 50 mmol (10.0 g) of 2-bromoacetyl bromide. The mixture was allowed to stir overnight and then diluted with 100 mL of tetrahydrofuran. After filtration to remove the generated TEA hydrobromide salt, the solvent was evaporated. The residue was then dissolved in 100 mL of chloroform and washed with 5% NaHCO$_3$ several times. After drying with anhydrous MgSO$_4$, it was heated to remove the solvent, and then the resulting bromide derivative was dried under vacuum for 24 h, generating a viscous, light brown liquid (yield: 4.52 g for PPGOH-1000 and 10.90 g for PPGOH-2500, 85%).

**Synthesis of PPG-Grafted Poly(amic acid-co-amic ester).** The graft copolymers were prepared in one-stage process. A 250-mL, two-necked flask, fitted with a nitrogen inlet was charged with 2.5 mmol (1.33 g) of diamine and 100 mL of dry NMP. The mixture was stirred to dissolve diamine, then the flask was cooled to 5°C and 2.5 mmol (1.13 g) of 6-FDA was added to it. After the resulting solution was allowed to heat to room temperature and stirred for 24 h, 0.55 mmol (0.007 g) of K$_2$CO$_3$, and 0.55 mmol of PPG-Br (0.0560 g of PPG Br-1000 or 0.131 g of PPG Br-2500) were added to the solution. The mixture was stirred for 48 h at room temperature. The obtained PPG-grafted poly(amic acid-co-amic ester) (PAAE-g-PPG) solution was precipitated into methanol/water (1:1 v/v) and methanol several times. The copolymer was dried under vacuum for 24 h at 40°C.

**Preparation of Polyimide Nanofoam.** A solution of PAAE-g-PPG was prepared by dissolving a copolymer in NMP or DMAC at a concentration of 7–10% solids. Thin film was
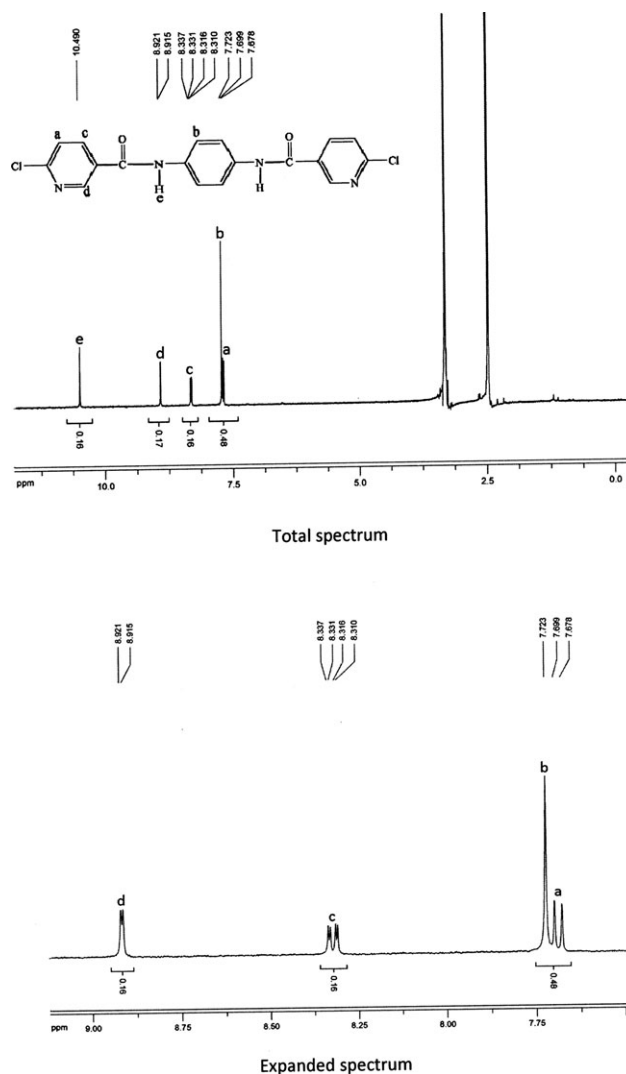


**Figure 1.** $^1$H-NMR spectrum of $N,N'$-(1,4-phenylene)bis(6-chloronicotinamide).
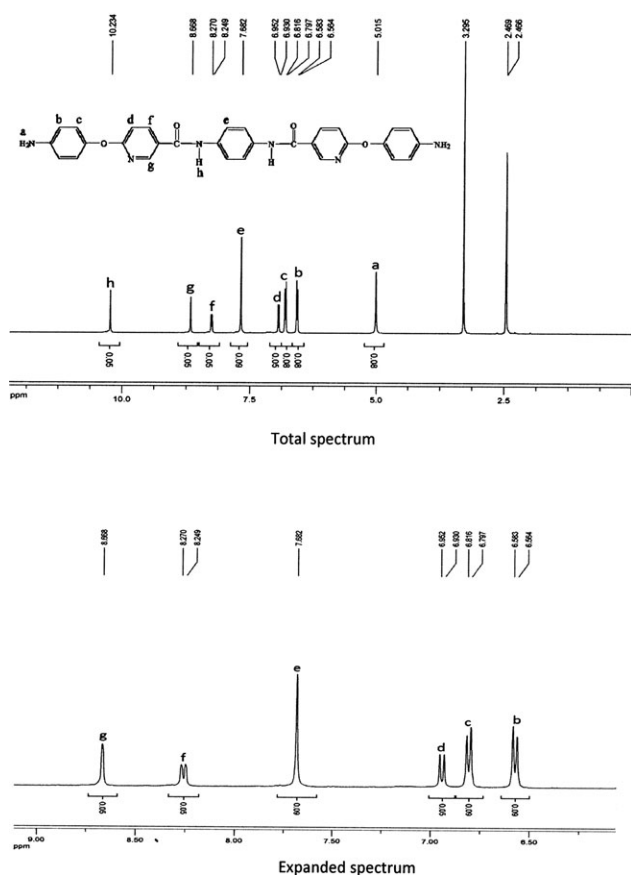
Total spectrum



Expanded spectrum

**Figure 2.** $^1$H-NMR spectrum of $N,N'$-(1,4-phenylene)bis(6-(4-aminophenoxy) nicotinamide.

formed by doctor blading (10–40 $\mu$m) on a glass plate. The polymer was heated incrementally to 180°C for 7 h under nitrogen atmosphere to eliminate the solvent and generated a polyimide film. Then it was heated at 260°C for 9 h in air atmosphere to obtain polyimide foam.

## RESULTS AND DISCUSSION

Preparation of polyimide foams with good solubility and low dielectric constant without sacrifice of their thermal and mechanical properties was the main aim of this study. Therefore, a new aromatic diamine was synthesized and used to produce polyimide nanofoams. This diamine was prepared via a two-step process. The first step involved a nucleophilic aromatic

substitution reaction of $p$-phenylene diamine with 6-chloronicotinoyl chloride in NMP to obtain a dichloro compound. The diamine monomer was readily obtained in the second step, through the aromatic nucleophilic substitution reaction of the dichloro compound with 4-aminophenol in the presence of $K_2CO_3$ and NMP (Scheme 1).

Structures of the dichloro compound and the diamine monomer were confirmed by common spectroscopic methods. In the FTIR spectrum, dichloro compound showed absorption bands of the functional groups at 3319, 1647, 1462 cm$^{-1}$ for amide N–H stretching, –C=O, and C=C bonds, respectively. In addition, absorption bands of diamine appeared at 3427, 1647, 1473, 1247 cm$^{-1}$ for amine N–H stretching, –C=O, C=C, and –O– bonds, respectively. The $^1$H-NMR spectrum of dichloro compound represented peaks at about 7.69 (d, 2H, pyridine), 7.72 (s, 4H, phenyl), 8.31 (dd, 2H, pyridine), 8.91 (d, 2H, pyridine), and 10.48 (s, 2H, amide) ppm. Also peaks at 5.01 (s, 4H, amine), 6.58 (d, 4H, phenyl), 6.79 (d, 4H, phenyl), 6.95 (d, 2H, pyridine), 7.68 (s, 4H, phenyl), 8.24 (dd, 2H, pyridine), 8.66 (d, 2H, pyridine), and 10.23 (s, 2H, amide) ppm were observed in $^1$H-NMR spectrum of the diamine. The $^1$H-NMR spectra confirmed that dichloro compound was completely converted into diamine by the high-field shift of the aromatic protons in the dichloro compound and appearance of signal at 5.01 ppm corresponding to the amino protons (Figures 1 and 2).

Two-step polycondensation reaction of the obtained diamine with hexafluoroisopropylidene diphthalic anhydride (6-FDA) as a commercially available aromatic dianhydride resulted in preparation of related poly(amic acid) and polyimide. The incorporation of ether and amide groups into the backbone of the diamine were quite effective to improve the flexibility of final polyimide film while the presence of pyridine ring (due to its aromaticity) and avoid of any weak linkages in the chemical structure of such diamine provided good thermostability in the final polyimide film.

High-temperature resistance polyimide nanofoams were also prepared from graft copolymers comprising of the polyimide matrix as a thermally stable block and a thermally labile dispersed block (PPG unites). The design was considered for production of foams with closed pores structure.

Hedrick et al.[23,27,29–32] have been extensively studied different labile blocks in these systems and gathered useful information. Poly (propylene glycol) was used as thermally decomposable coblock for this study, since it decomposes well below the Tg of
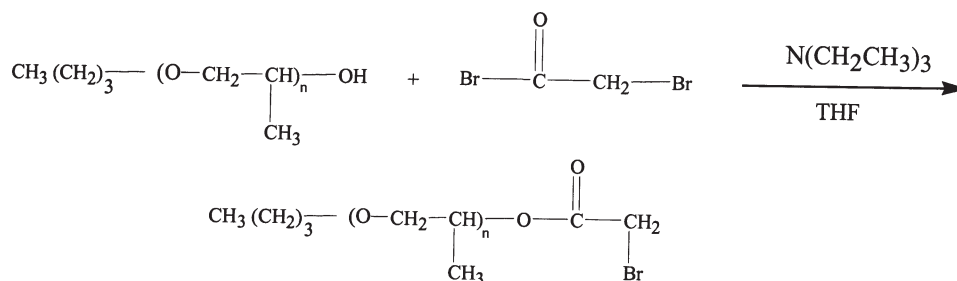


**Scheme 2.** Preparation of PPG-Br.
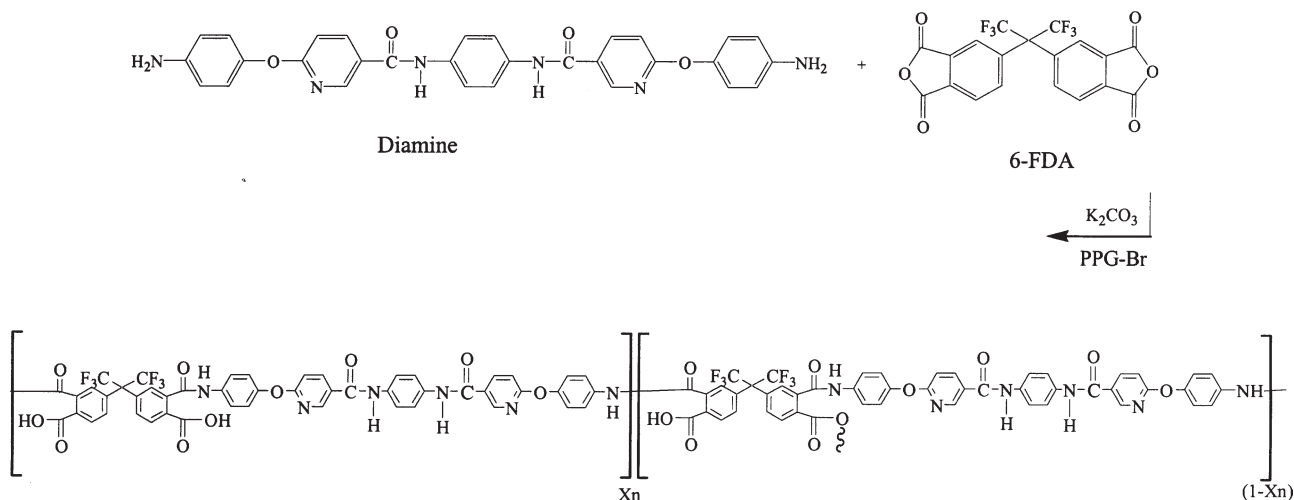
**Scheme 3.** Synthesis of PAAE-*g*-PPG.

the polyimide. The bromo-functional propylene glycol oligomers were prepared by the reaction of poly (propylene glycol) monobutyl ether with molecular weight of 1000 and 2500 g mol$^{-1}$ with 2-bromoacetyl bromide in the presence of TEA (Scheme 2).[33] The $^1$H-NMR spectra of these oligomers revealed a peak at about 3.98 ppm due to the generation of CH$_2$–Br bond. Poly(amic acid) for homopolymer was prepared by condensation of diamine with 6-FDA. The synthesis of copolymers was achieved by the addition of PPG-Br oligomers in the presence of K$_2$CO$_3$ to the poly(amic acid) solution. The resulting viscous solutions were precipitated in methanol/water (1 : 1 v/ v) and methanol several times to remove unreacted PPG-Br (Scheme 3). Since PPG-Br was soluble in methanol, precipitation and purification of PAAE-*g*-PPG in methanol was approved that PPG-Br was grafted onto PAA and it was not blended with PAA.[23,27]

The formation of PAAE-*g*-PPGs was assessed by FTIR and TGA techniques. The appearance of the peaks at about 2918–2926 cm$^{-1}$ and 1712–1720 cm$^{-1}$ for aliphatic C–H and ester groups,

respectively, approved the formation of PAAE-*g*-PPGs. Comparing FTIR spectra of PAA-*g*-PPG with PPG-Br showed that an absorption C–Br peak at about 560 cm$^{-1}$ in PPG-Br was disappeared in PAA-*g*-PPG spectrum, due to the formation of new C–O bond. This was another evidence for the grafting of PPG-Br onto PAA.

TGA of PAAE-*g*-PPG copolymers exhibited three-step decomposition behavior. The first weight loss at about 100°C might be attributed to the evaporation of water absorbed by hygroscopic structure of amic acids. The second weight loss was observed around 260°C due to the degradation of thermally labile PPG blocks and the third weight loss was begun above 400°C related to the thermal degradation of polyimide blocks. A representative TGA curve for PAAE-*g*-PPG (1000) was shown in Figure 3.

Thin films of diamine/6-FDA homopolymer and nanoporous structures were made by casting solutions of the polymer on the glass substrates. After the initial casting of pure poly(amic acid) without PPG unit, it was heated from 50 to 180°C at a heating rate of 20°C/h under air atmosphere and held at this temperature for 8 h to remove solvent of imidization process. The existence of characteristic peaks at about 1773, 1724 (imide –C=O–
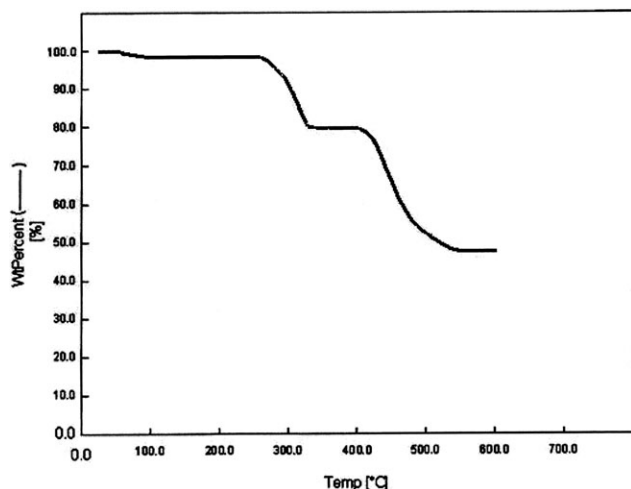


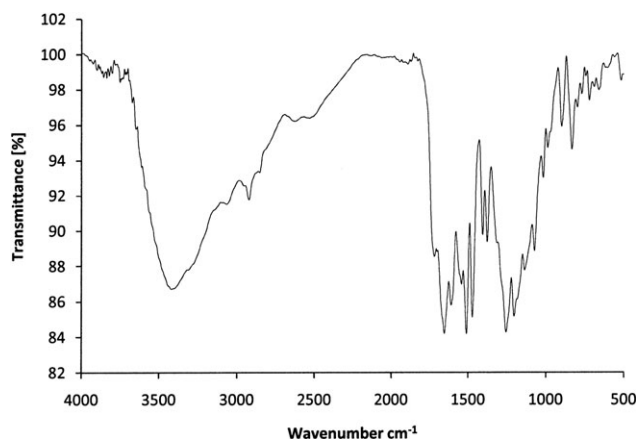**Figure 3.** TGA curve of PAAE-*g*-PPG (1000).



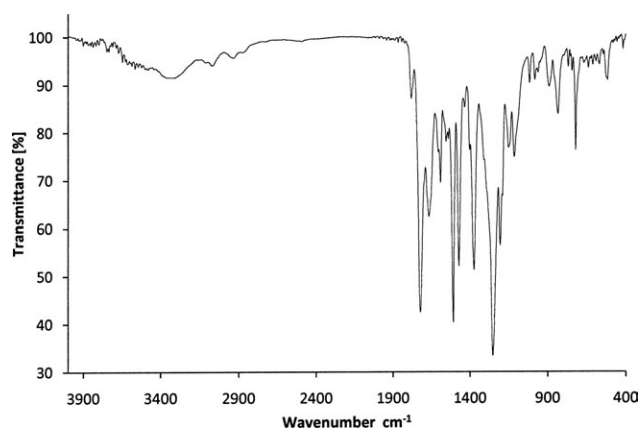**Figure 4.** FTIR spectrum of PAAE-*g*-PPG (1000).

**Figure 5.** FTIR spectrum of nanofoam (1000).

stretching), 1374 (imide –C–N stretching), and 723 cm$^{-1}$ (–C=O bending) in FTIR spectrum suggested the formation of imide ring in the polyimide film structure. It had to be mentioned that complete conversion of poly(amic acid) to polyimide was followed by FTIR spectroscopy. Disappearance of –OH band and appearance of four characteristic imide bands was observed in the FTIR spectrum after 8 h heating of poly(amic acid) solution at 180°C. So, it was concluded that although 1 h heating over 250°C has been reported for complete imidization, prolong heating (8 h) at lower temperature (180°C) would be sufficiently effective.

The poly(amic acid) samples with PPG unit were subjected in two thermal cycles. In this method, polymer solutions were heated from 50 to 180°C and held at 180°C for 8 h under nitrogen atmosphere for effective removal of solvent and subsequent imidization. Then they were heated at 260°C for 9 h under air atmosphere to remove PPG units and foam formation.

TGA results of nanofoams revealed no mass losses up to 335°C verifying complete elimination of PPG block. Moreover, FTIR spectroscopy confirmed that the peaks at about 2925 cm$^{-1}$ since C–H band of PPG were vanished (Figures 4 and 5).

The weight-average molecular weight ($M_w$) and number–average molecular weight ($M_n$) of polymers were measured based on GPC method. The obtained results for $M_w$, $M_n$, and polydispersity index (PDI) of polyimide and their nanofoams were collected in Table I.

The thermal stability of polymers was evaluated by TGA method. In general, nanofoam showed lower thermal stability than corresponding homopolymer due to the formation of pores. Polyimide

**Table I.** Molecular Weights of Polyimide and Nanofoams

| Polymer | $M_n$ | $M_w$ | PDI |
|---|---|---|---|
| Diamine—6FDA (h) | 45980 | 64370 | 1.40 |
| Diamine—6FDA-1000 (n) | 40200 | 65120 | 1.62 |
| Diamine—6FDA-2500 (n) | 41350 | 70300 | 1.70 |

h, Homopolymer; n, nanofoam.

**Table II.** Thermal Properties of the Polyimide and Nanofoams

| Polymer | $T_g$ (°C) | $T_0$ (°C) | $T_{10}$ (°C) | $T_{max}$ (°C) | Char yield at 600°C (%) |
|---|---|---|---|---|---|
| Diamine—6FDA (h) | 290 | 405 | 505 | 520 | 57 |
| Diamine—6FDA-1000 (n) | 248 | 335 | 455 | 505 | 50 |
| Diamine—6FDA-2500 (n) | 255 | 375 | 473 | 515 | 53 |

$T_0$, initial decomposition temperature; $T_{10}$, temperature for 10% weight loss; $T_{max}$, maximum decomposition temperature; Char yield, weight of polymer remained; h, homopolymer; n, nanofoam.

nanofoam that was derived from copolymer with the higher molecular weight of PPG-Br (2500) revealed higher thermal stability in comparison to polyimide nanofoam from PPG-Br (1000). This might be related to the more degradation of PPG-Br (1000) than PPG-Br (2500) in foaming thermal process.

The morphology of the copolymers before and after foaming was evaluated by DMTA technique. The temperature corresponding to the maximum peak value in tan$\delta$-T was considered as $T_g$ by DMTA analysis. Two clear $T_g$s were observed in their curves before foaming. The first $T_g$ was attributed to the contribution of PPG moieties which was very close to the $T_g$ of the initial poly (propylene glycol). The second one was related to the contribution of imide blocks in the structures. The phase purity of the copolymers was approved by these observations.[27]

In addition, the variations in glass transition behaviors of homopolymer and polyimide nanofoams were studied using DMTA method. The $T_g$ of porous films was less than the pure polyimide film. This can be due to the introduction of nanopores that increased the free volume of polymer, resulted in lowering of $T_g$. The results for polyimide and nanofoams were summarized in Table II.

Homopolymer and polyimide nanofoams were tested for tensile to verify the mechanical quality of the films. The drop in the tensile strength of nanofoams in comparison with homopolymer was due to the stress concentration caused by the nano-voids in the polyimide foams. Also, the tensile strength of polyimide

**Table III.** Tensile Strength, Dielectric Constant, Relative Pore Volume, and Density of Polyimide and Nanofoams

| Polymer | Tensile strength (MPa) | Dielectric constant | Pore volume (%) | Measured density (g/cm$^3$) |
|---|---|---|---|---|
| Diamine—6FDA (h) | 132 | 2.86 | – | 1.37 |
| Diamine—6FDA-1000 (n) | 112 | 2.29 | **15** | **1.67** |
| Diamine—6FDA-2500 (n) | 120 | 2.37 | 11 | 1.22 |

h, Homopolymer; n, nanofoam.

**Table IV.** Characteristic Features of the Foams

| Sample | Weight % PPG in reaction | Volume % PPG in reaction[a] | Weight % PPG after isolation[b] | Volume % PPG after isolation[a] | Volume fraction of pores[a,c] | Efficiency of process |
|---|---|---|---|---|---|---|
| 6FDA (1000) | 20 | 25 | 18 | 22 | 15 | More efficient |
| 6FDA (2500) | 16 | 20 | 14 | 17 | 11 | Less efficient |

[a]Determined by density, [b]Determined by TGA, [c]Determined by porosimeter.
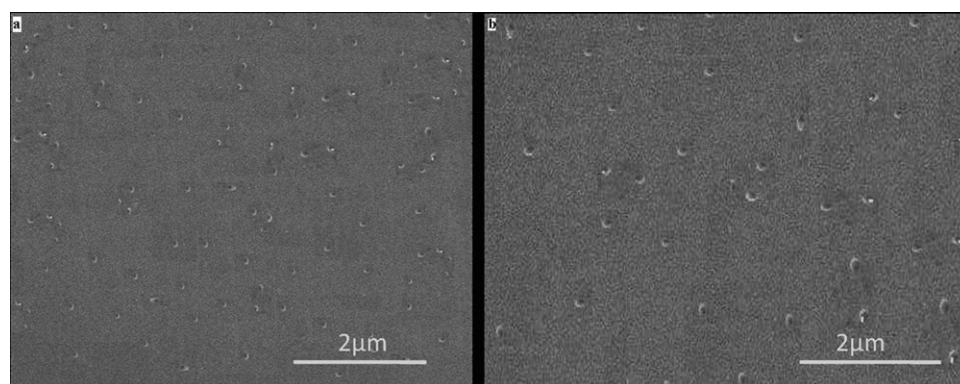


**Figure 6.** SEM image of (a) nanofoam (1000) and (b) nanofoam 2500.

nanofoams decreased with increasing the pores content. The data were summarized in Table III.

The dielectric constant values of pure polyimide film and nanoporous films at 1 MHz were presented in Table III. According to the obtained results, the dielectric constant of pure polyimide was about 2.86 whereas the dielectric constant of nanoporous polyimides with PPG-Br (1000) and PPG-Br (2500) were 2.29 and 2.37, respectively. It was clear that incorporating air pores into polyimide matrix lowered the dielectric constant efficiently. Apparently, incorporation of air pores into the polyimide backbone is more efficient for decreasing of the dielectric constant (2.29–2.37) in comparison to other methods like introduction of silane unit (2.46–2.92) into the backbone of polyimides.[15] In addition, the decreasing of dielectric constant was greater for nanofoam with higher porosity. The pore volume of the foams was determined based on the porosimeter measurement (Table III). The void formation and the free volume increase of the polyimide nanofoams were qualitatively verified by measuring their density (Table III).

To evaluate the efficiency of the process for the foam formation, some characteristic features of the polymers and related foams were determined using density, thermogarvimetric, and porosimeter measurements (Table IV). On the basis of the obtained data especially density data, it was found that partial foam collapsing was occurred in 2500-PPG foam.[24,29–32]

From SEM and TEM images, it was concluded that the porous structures formed nano-phase separated morphology with relatively uniform cellular structures. The average size of final pores was in the range of 30–60 nm and most of the pores were found in the form of closed cells (Figures 6 and 7).

## CONCLUSION

On the basis of the synthesis of a new pyridine-based ether diamine, a novel polyimide and related nanofoams were successfully prepared by grafting thermally labile PPG onto polyimide matrix. The chemical structures and properties of homopolymer
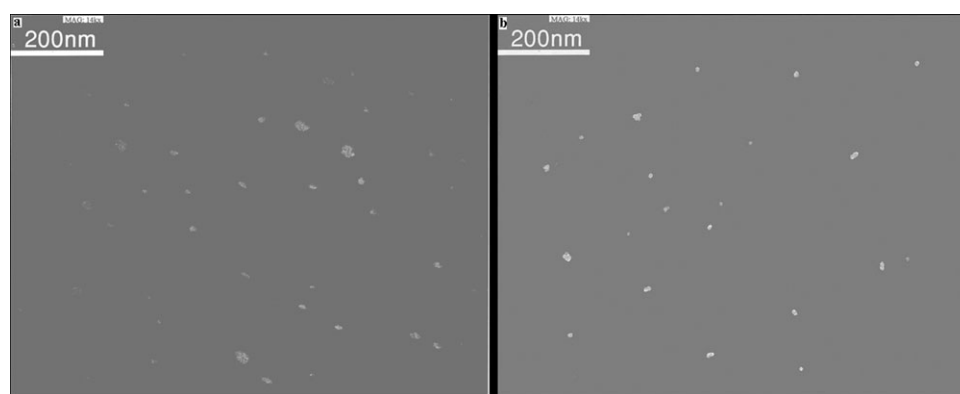


**Figure 7.** TEM image of (a) nanofoam (1000) and (b) nanofoam 2500.

and nanofoams were investigated by conventional methods. Although thermal stability of the polyimide nanofoams was slightly decreased in comparison to the polyimide, these nanofoams revealed lower dielectric constant than homopolymer due to the incorporation of voids. The combination of several properties resulted preparation of nanofoams as high-temperature resistant materials for electronic and microelectronic applications.

## REFERENCES

1. Ghosh, M. K.; Mittal, K. L. Polyimides: Fundamentals and Applications; Marcel Dekker, New York, **1996**.

2. Hergenrother, P. M.; Watson, K. A.; Smith, J. G.; Connel, J. W.; Yokota, R. *Polymer* **2002**, *43*, 5077.

3. Kim, T. Y.; Kim, W. J.; Lee, T. H.; Kim, J. E.; Suh, K. S. *eXPRESS Polym. Lett.* **2007**, *1*, 427.

4. Maier, G. *Prog. Polym. Sci.* **2001**, *26*, 3.

5. Mehdipour-Ataei, S.; Taremi, F. *J. Appl. Polym. Sci.* **2011**, *121*, 299.

6. Ragosta, G.; Musto, P. *Adv. Polym. Sci.* **2009**, *3*, 413.

7. Mittal, K. L. Polyimides: Synthesis, Characterization, and Applications; Plenum Press, New York, **1984**.

8. Mehdipour-Ataei, S.; Heidari, H. *J. Appl. Polym. Sci.* **2004**, *91*, 22.

9. Tan, L.; Liu, S.; Ling, Z.; Zhao, J. *Polym. Adv. Technol.* **2010**, *21*, 435.

10. Wang, C.; Zhao, X.; Li, G.; Jiang, J. *Polym. Degrad. Stab.* **2009**, *94*, 1746.

11. Choi, J. K.; Paek, K. Y.; Yoon, T. H. *Eur. Polym. J.* **2009**, *45*, 1652.

12. Mehdipour-Ataei, S.; Sarrafi, Y.; Hatami, M. *Eur. Polym. J.* **2005**, *41*, 2887.

13. Mehdipour-Ataei, S. *Eur. Polym. J.* **2005**, *41*, 91.

14. Mehdipour-Ataei, S.; Akbarian-Feizi, L. *Chinese J. Polym. Chem.* **2011**, *29*, 93.

15. Babanzadeh, S.; Mahjoub, A.; Mehdipour-Ataei, S. *Polym. Degrad. Stab.* **2010**, *95*, 2492.

16. Qiu, F. X.; Li, P. P.; Yang, D. Y. *eXPRESS Polym. Lett.* **2007**, *1*, 150.

17. Chol, K. H.; Lee, K. H.; Jung, J. C. *J. Polym. Sci. A Polym. Chem.* **2001**, *39*, 3818.

18. Mehdipour-Ataei, S.; Bahri-Laleh, N.; Amirshaghaghi, A. *Polym. Degrad. Stab.* **2006**, *91*, 2622.

19. Haidar, M.; Chenevey, E.; Vora, R. H.; Cooper, W.; Glick, A.; Jaffe, M. *Mater. Res. Soc. Symp. Proc.* **1991**, *35*, 227.

20. Hsiao, S. H.; Guo, W.; Chung, C. L.; Chen, W. T. *Eur. Polym. J.* **2010**, *46*, 1878.

21. Yang, C.-P.; Hsiao, S.-H.; Chung, C.-L. *Polym. Int.* **2005**, *54*, 716.

22. Tao, L.; Yang, H.; Liu, J.; Fan, L.; Yang, S. *Polymer* **2009**, *50*, 6009.

23. Hedrick, J. L.; Russell, T. P.; Labadie, J.; Lucas, M.; Swanson, S. *Polymer* **1995**, *36*, 2685.

24. Hedrick, J. L.; Charlier, Y.; Dipietro, R.; Jayaraman, S.; McGrath, J. E. *J. Polym. Sci. A Polym. Chem.* **1996**, *34*, 2867.

25. Jiang, L.; Liu, J.; Wu, D.; Li, H.; Jin, R. *Thin Solid Films* **2006**, *510*, 241.

26. Lee, Y. J.; Huang, J. M.; Kuo, S. W.; Chang, F. C. *Polymer* **2005**, *46*, 10056.

27. Charlier, Y.; Hedrick, J. L.; Russell, T. P.; Volksen, W. *Polymer* **1995**, *36*, 987.

28. Carter, K. R.; Dipietro, R.; Sanchez, M.; Swanson, S. S. *Chem. Mater.* **2001**, *13*, 213.

29. Hedrick, J. L.; Labdie, J.; Russell, T. P.; Hofer, D.; Wakharker, V. *Polymer* **1993**, *34*, 4717.

30. Hedrick, J. L.; Hawker, C. J.; Dipietro, R.; Jerome, R.; Charlier, Y. *Polymer* **1995**, *36*, 4855.

31. Hedrick, J. L.; Russell, T. P.; Sanchez, M.; DiPietro, R.; Swanson, S. S.; Mecerreyes, D.; Jerome R. *Macromolecules* **1996**, *29*, 3642.

32. Charlier, Y.; Hedrick, J. L.; Russell, T. P.; Swanson, S. S.; Sanchez, M.; Jérôme, R. *Polymer* **1995**, *36*, 1315.

33. Do, J. S., Zhu, B.; Han, S. H.; Nah, C.; Lee, M. H. *Polym. Int.* **2004**, *53*, 1040.